



HAL
open science

High resolution and High-Speed Atomic Force Microscope imaging

Francesca Zuttion, Lorena Redondo-Morata, Arin Marchesi, Ignacio Casuso

► **To cite this version:**

Francesca Zuttion, Lorena Redondo-Morata, Arin Marchesi, Ignacio Casuso. High resolution and High-Speed Atomic Force Microscope imaging. Yuri L. Lyubchenko. Nanoscale Imaging. Methods and protocols, 1814, Springer, pp.181-200, 2018, Methods in Molecular Biology, 978-1-4939-8590-6. 10.1007/978-1-4939-8591-3_11 . hal-01871339

HAL Id: hal-01871339

<https://hal.science/hal-01871339>

Submitted on 10 Sep 2018

HAL is a multi-disciplinary open access archive for the deposit and dissemination of scientific research documents, whether they are published or not. The documents may come from teaching and research institutions in France or abroad, or from public or private research centers.

L'archive ouverte pluridisciplinaire **HAL**, est destinée au dépôt et à la diffusion de documents scientifiques de niveau recherche, publiés ou non, émanant des établissements d'enseignement et de recherche français ou étrangers, des laboratoires publics ou privés.



Distributed under a Creative Commons Attribution 4.0 International License

Corresponding author information:

Dr Ignacio Casuso

e-mail: ignacio.casuso@inserm.fr

U1006 INSERM, Université Aix-Marseille, Parc Scientifique et Technologique de Luminy, 163
avenue de Luminy, 13009 Marseille, France.

High resolution & High-Speed Atomic Force Microscope imaging.

Authors: Francesca Zuttion, Lorena Redondo-Morata, Arin Marchesi, Ignacio Casuso*

Affiliation: U1006 INSERM, Université Aix-Marseille, Parc Scientifique et Technologique de Luminy, 163 avenue de Luminy, 13009 Marseille, France.

Running Head: HS-AFM Imaging

Abstract

The advent of high-speed atomic force microscopy (HS-AFM) in recent years has opened up new horizons for the study of structure, function and dynamics of biological molecules. HS-AFM is capable of 1000 times faster imaging than conventional AFM. This circumstance uniquely enables the observation of the dynamics of all the molecules present in the imaging area. In the last ten years, the HS-AFM has gone from a prototype-state technology that only a few labs in the world had access to (including ours) to an established commercialized technology that is present in tens of labs around the world.

In this protocol chapter we share with the readers our practical know-how on high resolution HS-AFM imaging.

Keywords

High Speed Atomic Force Microscope, HS-AFM, cantilever, Electron Beam Deposited tip, plasma EBD tip sharpening, tip-sample approach, oscillation amplitude, PID, feedback optimization, image treatment.

1. Introduction

The atomic force microscopy (AFM) [1] is a powerful tool for direct visualization of biological samples in an aqueous solution with sub-molecular resolution. It allows non-invasive imaging in physiological conditions of unlabeled biological samples, such as nucleic acids [2–4] and cell membrane proteins [5, 6]. AFM has rapidly emerged as an effective structural analysis tool,

complementing atomic structure data acquired by other techniques such as X-ray crystallography, NMR and electron microscopy. In contrast to these latter methods, which heavily rely on ensemble averaging, AFM exhibits a superior signal-to-noise ratio, enabling molecules to be observed individually under aqueous environment. To acquire a topographic image, a sharp tip attached to the free end of a flexible cantilever is brought into contact and scanned over a sample and its profile height is recorded over the selected scan area. The feedback control allows adjusting the force applied to the sample to avoid damaging fragile biological structures. As a result of the imaging process, during which the distance between the sample stage and the AFM probe varied following the sample topography, a 3D profilometric image of the sample surface is obtained. With the advantage of operating in nearly physiological conditions, AFM is an ideal platform to study biological dynamic processes at the molecular scale. Nevertheless, the framerate of one image every few minutes of conventional AFM is not sufficient to visualize most dynamic processes of biological molecules that take place in its majority at sub-second time scales. The introduction of the high-speed atomic force microscopy (HS-AFM) in 2001 opened the door to the visualization of biological molecule dynamics [7]. The technical development of the HS-AFM was performed by the laboratory of Toshio Ando in the University of Kanazawa, Japan.

HS-AFM allows imaging at maximum rates of 5-10 frames per second [8–11]. The operating principle of the HS-AFM is based on the miniaturization of the moving components of the AFM (cantilever and scanner) to increase their velocity by 1000 times, in the interest of achieving reaction speeds of tens of microseconds. For the HS-AFM probe, the gain in speed does not suppose a lost in performance. In the case of the scanner, the X,Y,Z displacement range is decreased $\sim 1:10$ over conventional AFMs. With this technique, centrosome [12, 13], DNA

origami [14], micelles [15] and many other biological systems have been imaged at high speed and high resolution.

In this book chapter, we describe in detail our HS-AFM imaging procedure for high resolution and high speed imaging, applicable to any version of the Ando-type HS-AFM system “SS-NEX”.

Such procedure is based on our experience imaging individual molecules [10, 16] or big macromolecular assemblies [17, 18].

2. Materials

2.1. High-Speed AFM

The protocol here described is adapted for any Ando-type HS-AFM setup “SS-NEX”, commercialized by the Research Institute of Biomolecule Metrology (RIBM), Japan. A picture of the HS-AFM hardware of our “SS-NEX” HS-AFM is presented in Figure 1, where the cantilever is mounted up-facing in a cantilever holder that comes with a pool of 110 μl while the sample is mounted on top of the scanner facing down. In general, imaging experiments are performed in tapping mode where the tip is oscillated at constant amplitude. For that, the cantilever is excited at its resonance frequency with the help of a miniaturized piezoelectric actuator. The sample can move in the XY-plane and also in the Z vertical direction thanks to three small multilayer piezoelectric actuators. The Z-piezo the one displaced at the highest frequency (nominal resonance frequency ~ 600 kHz and ~ 150 kHz once glued on the scanner). The deflection of the cantilever is monitored by an optical system. A laser beam with a 20x optical microscope objective is focused on the backside of the cantilever and the reflected beam tracked with a 15 MHz bandwidth photodiode which sends the signal to a Lock-In amplifier (Fourier Analyzer). The signal goes to the Proportional Integral Derivative (PID) controller which compares the amplitude readout with the value settled by the operator (set point amplitude, A) to feed

the adjustment of the clearance distance between the sample stage and the HS-AFM probe by the feedback loop.

2.2. Sample preparation and mounting

1. Glass-rod (small glass cylinder of 1.5 mm in diameter and 2 mm in height purchased from RIBM, Japan or SCHOTT, Switzerland), colorless nail polish (nitrocellulose dissolved in butyl acetate or ethyl acetate), mica sheet, puncher purchased from RIBM, cyanoacrylate glue (Super Glue®) or two components epoxy adhesive (Araldite®), adhesive tape (Scotch®), cellulose wipers (Kimwipes®), humid hood, microfuge tube of 1 ml.
2. HS-AFM probe: AC10 from Olympus ($f_c = 1.5$ MHz in air and $k_c = 0.1$ N/m) or USC-F1.5-k0.6 Nanoworld ($f_c = 1.5$ MHz in air and $k_c = 0.6$ N/m).
3. Optical microscope, tweezers, screwdrivers.
4. Rinsing solutions: anionic precision detergent cleaner (Alconox® dilute to 2% in water), ultrapure water (Milli-Q®), tap water, 70% ethanol, acetone.
5. Sample case: Supported Lipid Bilayer (SLB). Lipids: 1-palmitoyl-2-oleoyl-*sn*-glycero-3-phospho-(1'-*rac*-glycerol) (POPG), 1-palmitoyl-2-oleoyl-*sn*-glycero-3-phosphoethanolamine (POPE), chloroform, plastic tube (15 mL Falcon®), microfuge tube of 2 ml, Hamilton syringe, fume hood, vacuum desiccator, vacuum pump, potassium chloride, calcium chloride, working buffers: “liposome hydration buffer” 150 mM KCl, 10 mM Tris (tris(hydroxymethyl)aminomethane), pH 7.4 and “incubation buffer” 10 mM Hepes (4-(2-hydroxyethyl)-1-piperazineethanesulfonic acid), 100 mM NaCl, 5 mM CaCl₂, pH 7.4.

2.3. Plasma sharpening of the Electron Beam Deposited tips

1. A plasma system for surface treatment. We use a 40 kHz Diener ® Zepto system.

2. Piece of 2x1x1 cm³ of glass or Teflon.
3. Double sided carbon conductive tape.
4. Bottles of oxygen and helium gas.

2.4. Image treatment

1. Image processing software supplied with your AFM instrument (see Note 1).
2. MATLAB (MathWorks, USA). This is a proprietary programming language specifically designed for simple and efficient matrix manipulation, data plotting and algorithm implementation (see Note 2). A 30-day trial version is available for free download (<https://www.mathworks.com>). All the procedures described in section 3.5 can be carried out in MATLAB software environment. Routines written in this language for batch image processing described in section 3.5 are available at <https://sites.google.com/view/fm4b-lab/group-members/dr-arin-marchesi>.
3. ImageJ (NIH). This is a free, Java-based image processing platform (<https://imagej.nih.gov/ij/>). Although not specifically designed for AFM image treatment, a number of user-written plugins exists to efficiently tackle several of the procedures described in section 3.5. A routine written in MATLAB to convert the *.asd* HS-AFM file format in multipage 32-bit *.tiff* files supported by ImageJ is available at <https://sites.google.com/view/fm4b-lab/group-members/dr-arin-marchesi>.

3. Methods

3.1. Sample Preparation

1. Glue a cleaned glass-rod on the Z-piezo by using nail polish and let it dry for at least 20 min. Glass-rods can be cleaned by sonication ($f \sim 35$ kHz) in acetone and stored in a plastic box until use.
2. Glue a mica disk on the glass-rod with cyanoacrylate glue and let it dry for 10 min (see Note 3).
3. Cleave the mica disk with adhesive tape to obtain a clean, atomically flat surface. To facilitate the cleavage, mica can be previously cleaned with acetone (see Note 4).
4. Deposit a 1.2 μ l-2 μ l drop of the sample solution on the mica surface immediately after cleavage. Cover the sample with a humid hood to avoid drying (Figure 2, see Note 5).
5. Fill a cap of a microfuge tube of 1 ml with the working buffer solution (~ 300 μ l). Immerse the sample to wash it, this will remove the excess of molecules that did not adsorbed on the surface. Repeat the procedure at least five times without the need to replace the buffer between rinses.
6. Keep the sample wet with the working buffer solution under the humid hood until it is mounted on the HS-AFM.

3.2. Sample Mounting

1. Wash abundantly the cantilever holder with 2% anionic detergent, tap water, acetone, 70% ethanol and ultrapure water. Dry it gently with air or nitrogen flow if possible (see Note 6).
2. Set a small cantilever on the cantilever holder: position the cantilever on the trench of the cantilever holder and fix it with the cantilever holding screws (Figure 3, see Note 7).

3. Mount the cantilever holder on its base by placing the two magnets of the cantilever holder in contact with the micrometer screws of the base.
4. Wash the pool with 110 μ l ultrapure water for 10 times.
5. Fill the pool with 110 μ l of the working buffer.
6. Switch on the laser controller, select the “*I mode*” and adjust the intensity taking into account the SUM signal and the cantilever thermal fluctuation. This means that the chosen value should allow reaching a high SUM signal (in the range of 0.5-1.2 V) when the intensity of the reflected laser spot from the cantilever on the photodetector is maximized, while the thermal fluctuation of the cantilever is kept lower (in the range of 10 mV – 20 mV) (see Note 8).
7. Focus the cantilever on the camera screen and find the infrared laser spot ($\lambda = 808$ nm) (see Note 9).
8. Align the laser on the cantilever and adjust the photodiode parameters: use the micrometer screws of the cantilever holder base to adjust both the lateral and vertical positions of the holder until the intensity of the reflected laser spot from the cantilever on the photodetector is maximized. This corresponds to a maximum value of the SUM parameter on the photodetector controller. Set the DIFF parameter of the photodetector controller as close as possible to zero by using the Y-photodetector micrometer screw. In general, the SUM value should be around 0.5-1.2 V for new cantilevers.
9. Troubleshooting the laser alignment: If the SUM is too low, then check the position of the cantilever and try to adjust it. If the cantilever is not in focus point of the laser beam, modify its vertical position by using the Z-cantilever holder micrometer screw. The SUM will increase as the cantilever reaches the focus point

of the laser beam. If the laser spot is not well centered, use the XY-cantilever holder micrometer screws to adjust the lateral position of the cantilever. If the back of the cantilever is dirty or is an already-used cantilever then the SUM signal could be lower, in that case replace the cantilever.

10. Place the scanner holder. The scanner holder presents on the backside one linear and one circular grooves. The grooves have to be placed in correspondence with the support screws of the stage that determine the distance between the cantilever holder and the scanner. Ensure that the scanner holder is well positioned and does not move. Check the position of the screws of the scanner holder and ensure that they are retracted.
11. Carefully mount the sample scanner (Figure 4) on its holder by first accommodating the back (cable) side, putting the magnets in contact with the screws of the scanner holder and then placing the front side of the scanner. During this step, the sample will be plunged in the pool. Pay constant attention to the distance between the scanner and the cantilever while plunging in the sample, always looking at the video monitor. If they are too close to each other, then use the handy controller (“UP”) to move the step motors and lift up the scanner (see Note 10).
12. Check the alignment of the glass-rod and the cantilever by looking if the glass-rod is in the same vertical plane of the cantilever.
13. Connect the scanner to the break-out box (see Note 11).

3.3. Tip-sample approach in amplitude modulation mode

1. Before approaching the sample surface and the tip, check in the video monitor (video camera or CCD) that there are no bubbles around the surface or the AFM

chip (that would cause abnormal cantilever deflection). Likewise, ensure that in the camera display there are no particles or dust diffusing around in the liquid, due to contamination (see Note 12). The edges of both the sample support (mica, glass, *etc.*) and the cantilever should look clean.

2. The tip is placed relative to the sample stage around a millimeter away in the Z-axis, as shown in Figure 5A. In the camera display, the surface edge must be blurred or unfocused, ensuring that there is enough distance between the substrate surface and the cantilever (Figure 5B). Bring the sample close to the cantilever using the micrometer screws in XY-plane, as indicated by the arrow in Figure 5A.
3. In the Z-axis, bring the sample close to the cantilever performing a coarse approach with the Z-step motor (see Note 13). For approaching, the tip is exactly positioned in the vicinity of the edge of the surface (Figure 5C and 5D, see Note 14).
4. To find the first (or fundamental) resonance frequency of the cantilever, measure the thermal fluctuation of the HS-AFM probe cantilever performing a power spectrum of the photodiode signal (see Note 15).
5. Using the Fourier Analyzer, apply an AC sinusoidal voltage to the excitation piezo located on the cantilever holder, to excite the cantilever at the measured resonance frequency in point 3.4 (see Note 16).
6. Select the cantilever free amplitude between 0.1-0.5 V (see Note 17). This typically corresponds to amplitudes between 1-5 nm (see Note 18).
7. The amplitude set point of the cantilever should be lower than the free amplitude. In general, for the approach the amplitude set point is set around 20 % - 40 % lower than the free amplitude.

8. Ensure that everything is plugged, Z-scanner, isolation table (if used), X-, Y- and Z- drivers and PID are on (see Note 19).
9. Set parameters to start approaching: center the offset for the output voltage of the X-, Y-, and Z- drivers (see Note 20). In the PID controller: the integral gain is set typically at 20 % - 40 % of the maximum, the proportional and derivative gains are set to minimum. The tilt for the X- and Y- axes is also centered. If there are two time constants in the controller (slow and fast), switch to slow.
10. Approach automatically, selecting the velocity of the step motor and the percentage of amplitude reduction that will halt the automatic approach (see Note 21).
11. When the tip is very close to the surface, the free oscillation amplitude may vary significantly –usually increasing– due to unspecific interactions. If the oscillation amplitude varies, stop the automatic approach and readjust the set point amplitude 20 % - 40 % lower than the free amplitude. Proceed again to approach automatically.
12. If the software detects a tip-sample contact (when the set point amplitude approximates the free amplitude, detected thanks to the read-out of the amplitude and the PID output), the automatic approach stops automatically. In case of a manual approach, stop approaching when the Z-piezo starts to retract.
13. After the automatic approach stopped, offset the voltage of the piezo-driver until the output voltage in the PID is close to 0 V (see Note 22).
14. Troubleshooting the approach step: several situations may lead to an anomalous engage or a complete approach failure. It can be observed that the Z-piezo does

not hold the voltage value (it moves slowly to fully expanded or contracted position, or back and forth):

- a) Mica is not tightly attached to the glass-rod or the glass-rod is not firmly attached to the piezo stage. Sometimes mica partially exfoliates allowing some fluid leakage between the different layers. All these situations lead to oscillations of the surface while scanning that may prevent a successful approach.
- b) Due to a bad cleavage, or an excess of glue between the mica and the glass, the substrate plane is too inclined respect to the tip, hence the contact is not stable.
- c) The cantilever is tip-less (see Note 23). In this case, decreasing the amplitude set point also changes the SUM value in the photodetector (negative deflection values).
- d) There are big aggregates loosely adsorbed on the surface with strong and unspecific tip-sample interactions that vary the oscillation amplitude. Try to approach with lower amplitude set point, higher free oscillation amplitude or a different area; eventually reconsider the sample preparation.
- e) The solution is dusty or there is material adsorbing on the cantilever, which may lead to false engaging in the surface. Exchange the buffer solution in the pool or eventually increase the free oscillation amplitude. Eventually reconsider the sample preparation.

3.4. HS-AFM imaging

At this point the clearance distance between the sample stage and the HS-AFM probe is sufficiently small for the Z-piezo range to bring sample and the tip in and out of contact.

1. Out of contact, turn off the cantilever excitation, with the AFM probe, observe in the oscilloscope the width of the thermal vibration of the cantilever A_{Thermal} .
2. Turn on the excitation of the cantilever oscillation and set an out of contact oscillation $A_0 = 10 \cdot A_{\text{Thermal}}$.
3. Set a limited pixel number ($\sim 100 \times 100$ pixels), a set point amplitude $A > A_0$ so the tip is separated from sample, a small scan size ($\sim 50 \text{ nm} \times 50 \text{ nm}$), and a scan rate of 1 frame/second (see Note 24).
4. Start scanning, then slowly decrease the A , when it is below A_0 , the highest features on the sample are visualized. In the case of observing very high objects of hundreds of nanometer height that could damage the probe, move away to another region. If the area is appropriate for the HS-AFM tip to scan, decrease A a little more, so most of the area scanned is under slight tip contact.
5. Increase of the feedback speed: First, set the proportional (P) and the derivative (D) gains at their slowest possible reaction speed, next localize the integral (I) gain feedback speed saturation, for this increase the I gain slowly until strips of feedback resonance appear in the image (see Note 25), next reduce the I gain to a close to saturation position. If needed, the A can be slightly further decreased below A_0 to obtain an optimal surface profile. Typical A values range from $0.90 \cdot A_0$ to $0.5 \cdot A_0$. In the case of having several time constants in the controller it is possible that you may have to switch to the fastest reaction speed one to achieve the I gain saturation. Specific PID values are not given as they will depend on the gain adjustments of the rest of the feedback loop.

6. Localization of 'area of interest': Increase the scan area progressively to several hundred nanometers and increase the number of pixels accordingly. It is recommended to have between 1 and 2 pixels per nanometer. Look for the area of interest where to perform the imaging, displacing on the sample using the sample stage. Use always minimal force (maximal possible set point amplitude A) for imaging to reduce the risk of tip damage. In the case that it is not found an area of sufficient interest in the available scan area, withdraw the sample from the tip, displace macroscopically using the screws and approach on other area (see Note 26).
7. In the case you localize an area of interest, zoom in to frame your experiment, the frame should show clearly all the areas that are important for posterior data analysis.
8. Optimization of oscillation amplitude: Reduce the amplitude excitation signal, the probe will go out of contact, reduce the set point amplitude A to regain tip-sample contact, further reduce the excitation signal, further reduce A ... repeat this procedure until you arrive to a cantilever oscillation that is $A_0 \sim 5 \cdot A_{\text{Thermal}}$.
9. Check again the feedback saturation limit position by increasing the feedback speed of the I gain, next slow down slightly the I gain to avoid feedback resonance, and next increase the feedback speed of the P gain parameter to increase contrast on fine topographic details.
10. Speed increase: progressively increase the imaging speed, evaluate the loss of quality on the image relative to speed increase. Select the speed that provides a fair compromise between image quality and maximum possible speed.

11. If the sample presents height jumps over a few nanometers, the standard PID feedback speed of reaction may be too slow to correctly contour the sample during downhill scanning (so-called parachuting), in this case the HS-AFM dynamic PID should be turned on [19].
12. Dynamic PID tuning: set all values to 0 (the upper threshold, the lower threshold, and their corresponding gains). Slow down the imaging rate to its lowest speed where parachuting is observed. Next, increase the gain of the upper threshold until the parachuting disappears. Next, increase the imaging speed until parachuting reappears and again increase the gain of the upper threshold until the parachuting disappears. Repeat this action until resonances start appearing in the imaging, then reduce slightly. The gain of the lower threshold is usually set to 0 unless the sample shows very sharp uphill slopes (for example, trenches).
13. The shape of the tip apex is the most important parameter regarding the resolution. If the resolution obtained is not satisfactory, tip sharpening of the amorphous carbon tip deposited by electron beam deposited (EBD) on the end of the small cantilever is advised, for this use the gas plasma chamber.
 - i) In a piece of clean glass or Teflon, place on the border a strip of double sided carbon tape. Position the HS-AFM probe in a way that only the cantilever chip is in contact with the carbon tape, hence the cantilever and its tip are poked out in the air (see Note 27).
 - ii) Introduce the HS-AFM cantilever probe with its support in the plasma chamber of the plasma. Select the gas to fill in the chamber (see Note 28). Run the plasma chamber for a few tens of seconds, inert gases require longer times. Typical parameters we use are pressure ~ 1 mbar, power ~ 20 W.

iii) Image the sample with the sharpened tip. If resolution is not good enough further repeat steps i) to iii). Figure 6 shows the image quality improvement on Outer Membrane Porin F (OmpF) following consecutive sharpening cycles (see Note 29).

3.5. HS-AFM video processing and displaying

HS-AFM produces large data sets of image sequences that are affected by a number of instrument-specific peculiarities (such as drift of the piezoelectric elements, contrast discontinuities along the fast- and slow-scan axes, feedback parameters, etc.) that need to be accounted for before any analysis is performed.

Hereafter we provide some clues and suggestions in order to fix these instrument-specific hitches in what we believe is an accurate and time effective manner.

1. Open the HS-AFM data file with your favourite AFM software or programming language. Our own routine to read *.asd* HS-AFM file formats in MATLAB is available at <https://sites.google.com/view/fm4b-lab/group-members/dr-arin-marchesi>. To normalize the brightness across all the image stack subtract from each frame the frame average intensity (see Note 30).
2. Visually inspect your image stack and remove all the corrupted frames eventually present (changes in imaging conditions might result in insufficient forces or even the tip being for a certain amount of time out-of-contact). You might also consider removing frames skewed or dilated by sudden and fast motions of the scanner or sample.
3. Align all the frames in the stack to a reference image (see Note 31) in order to compensate for X- and Y-axis drift (see Note 32). This can be first tried in an automated way using normalized cross-correlation (or other image registration

algorithms) and reiterated throughout all the frames using control flow statements (see Note 33). Visually inspect the aligned image stack and delete -or manually overlay- badly registered frames to the reference image.

4. Remove X- and Y-axis tilting by means of three-point plane fitting (see Note 34). To attain this, first filter each frame with a 2D Gaussian blur filter to remove high frequency noise. Afterwards, identify three points that sit on the substrate/background of the image. Make sure these very same points are on the substrate only throughout all the frames. Fit each triad with a plane and subtract it from the aligned video.
5. Perform a horizontal line-by-line levelling (see Note 35). As the background has been already subtracted, a median (0 order) levelling will suffice (see Note 36). To avoid levelling artefacts make sure to exclude features not belonging to the substrate/background (usually by means of their height) from the computation. Define a region of interest over the substrate and fit the histogram with a Gaussian function to verify that the variance of the background has decreased after the procedure.
6. Fine align all the frames in the stack to a reference image using sub-pixel precision. For this purpose a software package that performs template matching by means of zero mean normalized cross-correlation was developed by our group some time ago [20]. Alternatively, use the ImageJ plugin Template Matching and Slice Alignment (see Note 32).
7. (Optional) Filter frame by frame the image stack with a matrix Gaussian filter to remove unwanted high-frequency noise. Be aware that over-application of low-pass filters or use of large matrices will tend to blur the data.

4. Notes

1. Although AFM image processing and analysis is in general best done with the software supplied by the instrument manufacturer, software packages provided with HS-AFM instruments might be rather limited, and more powerful third party packages are often needed.
2. Alternatively, a free software compatible with many MATLAB scripts is GNU Octave (<https://www.gnu.org/software/octave/>). All the procedures described in section 3.5 can be implemented in Octave.
3. Mica disks with a diameter of 1.5 mm are used as sample surfaces. To obtain them, ~ 0.05 mm thick mica sheets are perforated with a puncher. Careful attention must be paid in the selection of the mica disk. The disk should present a regular and flat border since only areas near the edges will be used for imaging. For gluing the mica disk on the glass-rod it can be used whether cyanoacrylate adhesive or a two-components epoxy adhesive.
4. To facilitate the cleaving of the mica disk glued on the glass-rod, you can clean the surface with a cellulose wipe soaked with acetone before performing the cleavage. Acetone can eliminate possible residues of organic material from previous sample preparation and facilitate the attachment of the adhesive tape on the mica sheet that will be removed. The final surface will not be affected by the previous use of acetone.
5. Use a wet cellulose wipe to create a humid environment inside the hood. Incubation conditions (time, temperature, etc.) will depend on the sample type.
Sample case: Preparation of supported lipid bilayers (SLBs) on mica. POPG and POPE lipid stocks are kept in solution in chloroform. The stock solutions are

mixed in a microfuge tube of 2 ml to obtain the desired molar ratio and diluted in chloroform:methanol (3:1, v:v). The organic solvent is evaporated under a gentle nitrogen flow. After the sample is kept in a desiccator under reduced pressure overnight. The “liposome hydration buffer” is heated up at 65 °C and it is used to rehydrate the sample. Then, the sample is dropped in a thermal bath at 65 °C for 45 s, following by 45 s vortexing; this heating-vortexing cycle is repeated 5 times. Finally, the lipid suspension is sonicated for 30 min in an ultrasonic bath ($f \sim 35$ kHz) to obtain large unilamellar vesicles. 1 μ l of the “incubation buffer” and 1 μ l liposomes suspension are incubated at room temperature on a freshly cleaved mica under a humid hood for 20 min. The sample is then rinsed 10 times with imaging buffer and then imaged by HS-AFM.

6. Pay attention not to wet the backside of the cantilever holder.
7. To settle the cantilever, completely remove the plate and position the cantilever, then first secure the screw at the bottom of the plate and afterwards the one in the front (see Figure 3). Do not screw too strong, screws can break easily, but enough to ensure the tight fit of the cantilever and avoid possible vibration during imaging. Alternatively, slide the cantilever into place with the help of tweezers to rise up the plate and secure the screws as explained before. Pay attention not to damage the cantilever during this operation. The cantilever must be parallel to the holder otherwise it would be easier to break it when mounted on the setup. For imaging experiment, the small cantilever listed in the “*Material*” section should be used.
8. Imaging experiments can be performed with the laser diode driver set in constant intensity “*I mode*” or constant power “*P mode*”, depending on the type of sample

and conditions in which to be imaged. For high-resolution imaging, we recommend using the laser diode driver in the “*I mode*”. The “*P mode*” operates a feedback system that may introduce noise to the image. It can be used to avoid local heating when performing one-day long measurements.

Characteristic values we use are: in the “*I mode*”, set the output between 21.8 and 23 mA, while in the “*P mode*” set the output between 0.13 and 0.18 mW for the laser diodes used in HS-AFM, although this number may vary with the ageing of the laser diode.

9. To facilitate this task, set the video camera in high light sensitivity (“*night shot*” mode) so the laser spot is intensified and easily visible on the screen.
10. In the case the wide XY range scanner (scan range: $XY = 4 \mu\text{m} \times 4 \mu\text{m}$, $Z = 0.7 \mu\text{m}$) is used to perform imaging experiments, the screws of the scanner holder are in the front side of the element. Also in this case, to accommodate the scanner, the backside is first positioned and afterwards the front side is placed by engaging the magnets in contact with the screws.
11. Before connecting the scanner, check the liquid in the pool neither to form a pronounced meniscus nor wet the Z-scanner, because while applying a voltage during imaging may cause an electric arc and consequently damage the Z-scanner.
12. If the fluid in the pool does not look clear or there are particles, dust visible in the video monitor, renew your buffer solution exchanging the fluid several times in the chamber. If the problem persists, consider these situations: i) the adsorption of the sample to the surface is not strong enough, ii) the sample concentration is too high, iii) there is a possible buffer solution-sample interaction (for example, magnesium salts precipitate in phosphate buffer).

13. To prevent the tip crashing on the surface, it is critically to be very attentive to the video camera while performing a coarse approach. Stop the coarse approach when the surface edge starts to define but is still blurred or unfocused. If the tip crashes brutally on the surface it will be most likely damaged.
14. The cantilever position on the surface is important for high-speed imaging. If the cantilever is not placed in the edge but closer to the middle area of the surface, during imaging, the Z-scanner exerts a viscous drag or a hydrodynamic pressure that drags the base or chip of the cantilever, which leads to an increase in the response time and imprecise cantilever deflection [8, 21, 22].
15. Usually, AFM operating software programs include this function.
16. The fundamental resonant frequency is convoluted when using piezo acoustic excitation of the cantilever with a myriad of peaks due to ‘echoes’ in the liquid cell pool, the so-called *the forest of peaks*. HS-AFM imaging is performed selecting a frequency that ‘echoes’ in the fluid cell in the range of frequencies of the fundamental resonance of the cantilever [23].
17. Typically, the free oscillation amplitude is set in concordance of the roughness of the sample; the flatter the sample; the lower the amplitude.
18. To convert the amplitude value from V to nm, it should be calibrated once approached using the optical beam detection sensitivity, which requires performing force curves (approach and retract cycles between the tip and the sample). In general, avoid calibrating the sensitivity before imaging –or before the experiment– to prevent tip damage or tip wearing. The calibration can be performed at the end of the experiment, after imaging. At this step –to approach–

use an approximate value: the sensitivity does not change significantly for the same type of cantilevers.

19. When the PID controller is **active** and the amplitude set point is set lower than the free oscillation amplitude, the Z-piezo fully expands (to positive voltage).
20. If the full voltage range of the Z-piezo driver is 50 V, center it to 25 V. If the full voltage range of the X- and Y- piezo drivers are 100 V, center them to 50 V.
21. A typical percentage of amplitude reduction for halting the automatic approach is ~30 %. Alternatively, manually approach slowly moving the step-motor to bring close the cantilever to the sample surface. This is particularly useful when the surface is rough and/or heterogeneous.
22. Alternatively, slowly up or down with the step-motor.
23. In general for high-resolution imaging, it is very common to use amorphous carbon or carbon nanofibers tips. These materials are brittle and therefore they break easily. Always scan with very gentle tapping.
24. During the first images the risk of tip damage is high, here it is intended to limit it.
25. If the integral I gain is increased too much, saturation of the feedback loop bandwidth occurs; the Z-displacement cannot be done any faster even if the PID controller is requiring it. Then when I saturation is reached the feedback loop breaks, and error accumulates in the integrator-circuit, an I signal overshoot is created. Next, the circuit will create to compensate an overshoot of the I signal in the other direction. This oscillatory sequence of overshoots creates strips in the topographic image of the HS-AFM. Importantly, the I saturation depends on the topography of the sample under the tip. I saturates on the sample topographies that demand faster motions of the z-displacement, the uphill and downhill motions.

26. To avoid tip damage during the withdraw, first retract the tip from the sample using the Z-piezo displacement; for this set point $A > A_0$ before using the motor.
27. Otherwise, as surfaces get charged with plasma, the cantilever can break due to electrostatic repulsions.
28. The nature of the gas injected in the plasma chamber affects the etching rate of the amorphous carbon EBD tip. For example, oxygen oxidizes the carbon or the EBD tip, hence is more aggressive than inert gases such as helium, whose atoms just physically bombard the carbon. As a general rule, the less is the imaging resolution, the more etching power should be applied on the tip apex.
29. The final shape of the sharpened apex depends on its initial shape, high resolution apexes are not achievable always by plasma etching, a minimum of sharpness of the initial apex is required. So, in the case that after a few cycles of sharpening the required resolution is not achieved, the HS-AFM probe should be replaced.
30. This operation can be implemented in few simple steps using a *for* loop. Routines to perform in MATLAB this and other described processing steps are freely available at <https://sites.google.com/view/fm4b-lab/group-members/dr-arin-marchesi>.
31. The performance of image registration also depends upon the choice of the reference image (template). To increase the signal-to-noise ratio you shall build your reference image by averaging over several frames (usually 10-20). For this purpose, we recommend to use the median, which is more robust than the mean. Cropping is also commonly used to remove unwanted features from the edges of the averaged image.

32. Mechanical and piezo-scanner drifts may result into movies in which the sequential frames are not perfect real-space superposition. Therefore, before any data can be extracted from a HS-AFM image stack, all images must be perfectly aligned with respect to a stable coordinate origin.
33. For this purpose, an excellent option is the ImageJ plugins Template Matching and Slice Alignment (available at <https://sites.google.com/site/qingzongtseng/template-matching-ij-plugin>). Please note that this routine requires your video to be converted in 16-bit format, which might result in an unwanted loss of information. If this is the case, discard the obtained aligned video and apply the computed X and Y shifts to your original image stack to create a new registered image stack.
34. Nonlinearities of the piezoelectric scanners to the applied voltage can result in curved trajectories of the probe or sample stage (depending on the configuration of your system). If scanner bow artefacts are present, you shall consider fitting your image stack with a second order polynomial surface through five points.
35. As the horizontal axis is usually the fast scan axis, any change in imaging conditions over the time of the scan will lead to horizontal discontinuities in the topographs. It will thus be well accounted for by a horizontal line-by-line levelling.
36. In this routine, for each row of the image, the row median is subtracted from every element in the row.

Acknowledgements

This work was supported by French National Institute of Health and Medical Research (Inserm); the program "Investissements d'Avenir" by the French National Research Agency, ANR-10-

LABX-0083 (Labex EFL); Grant ANR-16-CE15-0023 (ANR SalmoTubes); Grant ANR-15-CE11-0020 (ANR MoBaRhE). A.M acknowledges support from the Long Term EMBO Fellowship (ALTF 1427-2014) and the Marie Curie Action (MSCA-IF-2014-EF-655157).

References

1. Binnig G, Quate CF (1986) Atomic Force Microscopy. *Phys Rev Lett* 56:930–933.
2. Ido S, Kimura K, Oyabu N, Kobayashi K, Tsukada M, Matsushige K, Yamada H (2013) Beyond the helix pitch: Direct visualization of native DNA in aqueous solution. *ACS Nano* 7:1817–1822.
3. Ares P, Fuentes-Perez MEE, Herrero-Galan E, Valpuesta JMM, Gil A, Gomez-Herrero J, Moreno-Herrero F (2016) High resolution Atomic Force Microscopy of double-stranded RNA. *Nanoscale* 8:11818–11826.
4. Hansma HG, Vesenka J, Siegerist C, Kelderman G, Morrett H, Sinsheimer RL, Elings V, Bustamante C, Hansma PK (1992) Reproducible Imaging and Dissection of Plasmid DNA Under Liquid with the Atomic Force Microscope. *Science* (80-) 256:1180–1184.
5. Henderson E, Haydon PG, Sakaguchi DS (1992) Actin Filament Dynamics in Living Glial Cells Imaged by Atomic Force Microscopy. *Science* 257:1944–1946.
6. Schabert F, Henn C, Engel A (1995) Native Escherichia coli OmpF porin surfaces probed by atomic force microscopy. *Science* (80-) 268:92–94.
7. Ando T, Kodera N, Takai E, Maruyama D, Saito K, Toda A (2001) A High-speed Atomic Force Microscope for Studying Biological Macromolecules. *PNAS* 98:124688–12472.
8. Ando T, Kodera N, Maruyama D, Takai E, Saito K, Toda A (2002) A High-speed Atomic Force Microscope for Studying Biological Macromolecules in Action. *Jpn J Appl Phys* 41:4851–4856.
9. Ando T, Uchihashi T, Kodera N (2013) High-speed AFM and applications to biomolecular

- systems. *Annu Rev Biophys* 42:393–414.
10. Casuso I, Khao J, Chami M, Paul-Gilloteaux P, Husain M, Duneau J-P, Stahlberg H, Sturgis JN, Scheuring S (2012) Characterization of the motion of membrane proteins using high-speed atomic force microscopy. *Nat Nanotechnol* 7:525–529.
 11. Ando T (2012) High-speed atomic force microscopy coming of age. *Nanotechnology* 23:62001.
 12. Gorle S, Pan Y, Sun Z, Shlyakhtenko LS, Harris RS, Lyubchenko YL, Vukovic L (2017) Computational Model and Dynamics of Monomeric Full-Length APOBEC3G. *ACS Cent. Sci.*
 13. Pan Y, Sun Z, Maiti A, Kanai T, Matsuo H, Li M, Harris RS, Shlyakhtenko LS, Lyubchenko YL (2017) Nanoscale Characterization of Interaction of APOBEC3G with RNA. *Biochemistry* 56:1473–1481.
 14. Rajendran A, Endo M, Katsuda Y, Hidaka K, Sugiyama H (2011) Programmed Two-Dimensional Self-Assembly of Multiple DNA Origami Jigsaw Pieces. *ACS Nano* 5:665–671.
 15. Inoue S, Uchihashi T, Yamamoto D, Ando T (2011) Direct observation of surfactant aggregate behavior on a mica surface using high-speed atomic force microscopy. *Chem Commun* 47:4974.
 16. Munguira I, Casuso I, Takahashi H, Rico F, Miyagi A, Chami M, Scheuring S (2016) Glasslike Membrane Protein Diffusion in a Crowded Membrane. *ACS Nano* 10:2584–2590.
 17. Chiaruttini N, Redondo-Morata L, Colom A, Humbert F, Lenz M, Scheuring S, Roux A (2015) Relaxation of Loaded ESCRT-III Spiral Springs Drives Membrane Deformation. *Cell* 163:866–879.

18. Mierzwa BE, Chiaruttini N, Redondo-Morata L, Moser von Filseck J, König J, Larios J, Poser I, Müller-Reichert T, Scheuring S, Roux A, Gerlich DW (2017) Dynamic subunit turnover in ESCRT-III assemblies is regulated by Vps4 to mediate membrane remodelling during cytokinesis. *Nat Cell Biol* 19:787–798.
19. Kodera N, Sakashita M, Ando T (2006) Dynamic proportional-integral-differential controller for high-speed atomic force microscopy. *Rev Sci Instrum* 77:83704.
20. Husain M, Boudier T, Paul-Gilloteaux P, Casuso I, Scheuring S (2012) Software for drift compensation, particle tracking and particle analysis of high-speed atomic force microscopy image series. *J Mol Recognit* 25:292–298.
21. Ando T, Uchihashi T, Scheuring S (2014) Filming biomolecular processes by high-speed atomic force microscopy. *Chem Rev* 114:3120–3188.
22. Uchihashi T, Kodera N, Ando T (2012) Guide to video recording of structure dynamics and dynamic processes of proteins by high-speed atomic force microscopy. *Nat Protoc* 7:1193–1206.
23. Carrasco C, Ares P, De Pablo PJ, Gómez-Herrero J (2008) Cutting down the forest of peaks in acoustic dynamic atomic force microscopy in liquid. *Rev Sci Instrum* 79:111–113.

Figure captions:

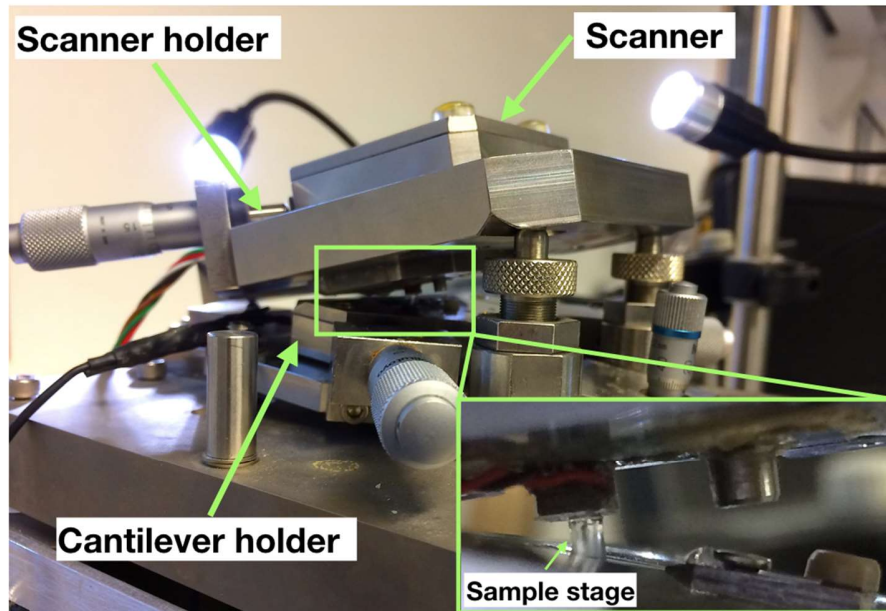


Figure 1: **HS-AFM hardware.** Image of the HS-AFM hardware. Relevant parts are signaled: the scanner, the scanner holder and the cantilever holder are shown. Right, zoom-in of the HS-AFM hardware, where the sample stage is plunged in the pool, above the cantilever.

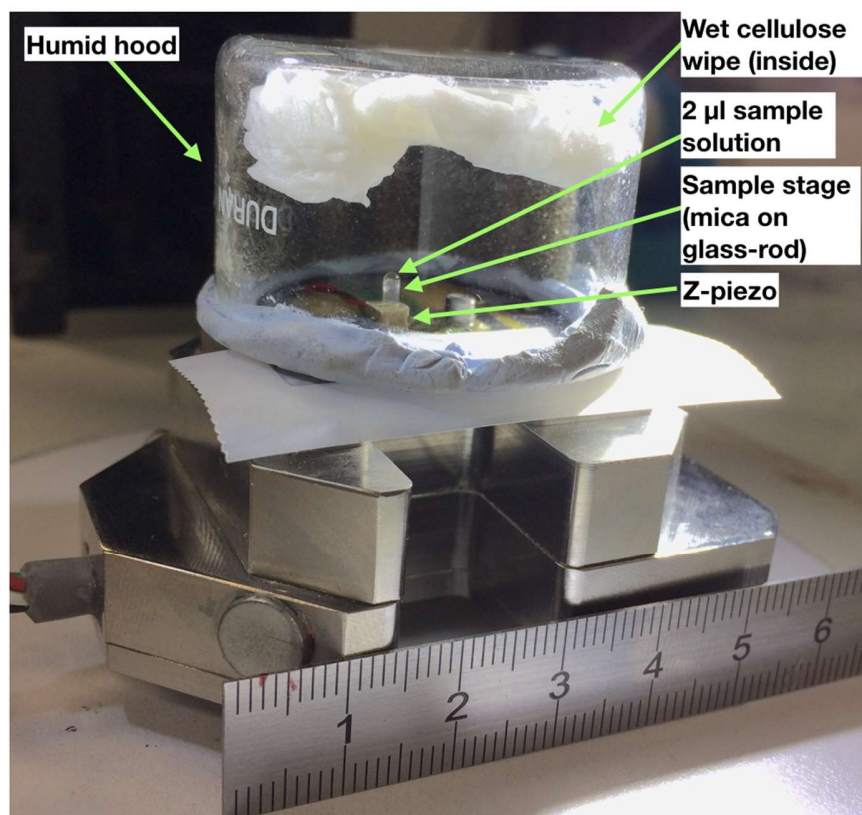


Figure 2: **Sample Incubation.** Image of the humid hood used for sample incubation on a sample stage (mica disk glued on the glass rod) attached to the Z-piezo of the scanner. The humid ambient is kept by a wet cellulose wipe inserted in the hood.

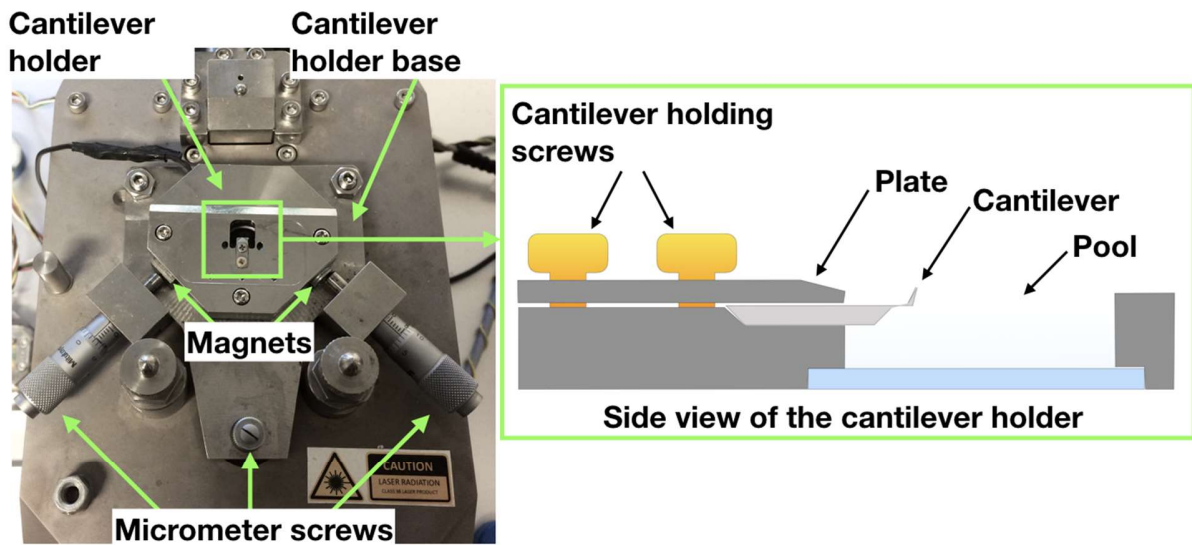


Figure 3: **HS-AFM cantilever holder**. Left, top view of the high-speed cantilever holder, showing how the cantilever holder is positioned on the cantilever holder base and the micrometer screws. Right, sketch of the side view of the chip cantilever holder, showing the cantilever holding screws, the plate, a side view of the chip with its cantilever and the pool filled with aqueous solution.

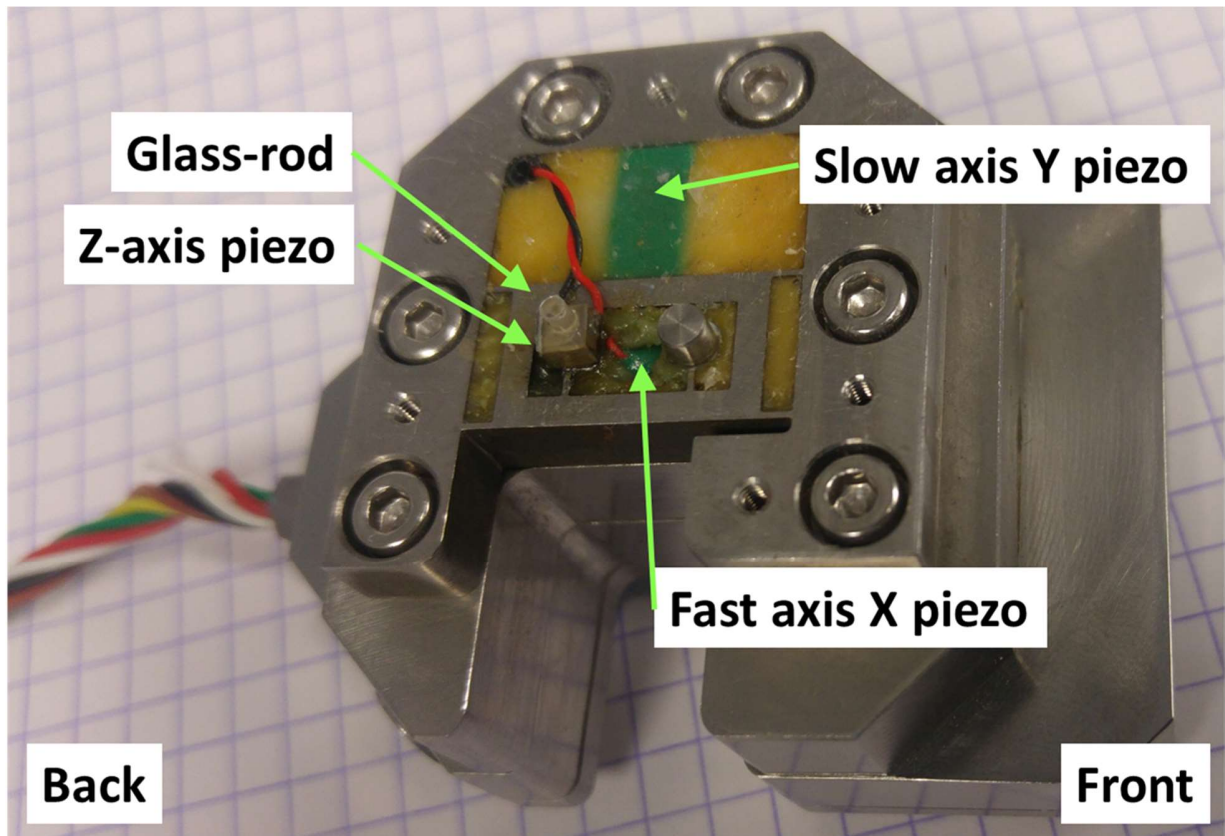


Figure 4. **HS-AFM sample scanner**. Image of the standard HS-AFM sample scanner. Relevant parts are signaled: slow axis Y piezoelectric actuator, fast axis X piezoelectric actuator, Z-axis piezoelectric actuator, and the glass-rod where the mica disk substrate is glued.

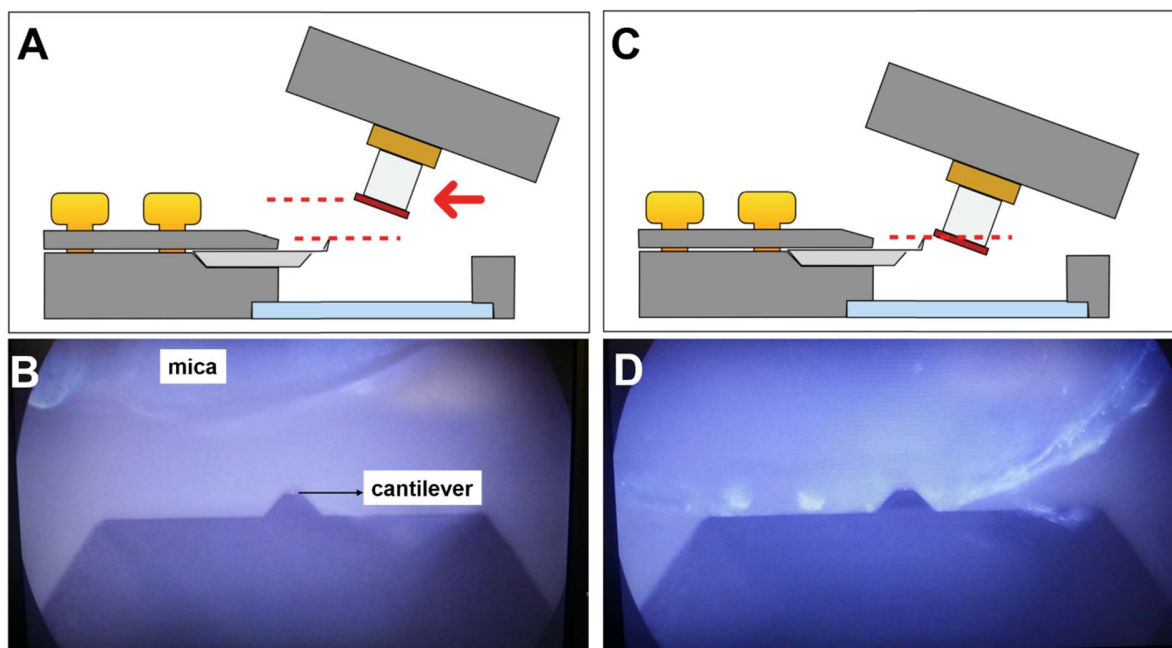


Figure 5. **Cantilever-sample positioning for approaching.** A) Scheme of the cantilever holder and the sample stage before approaching (side view). The mica surface is placed ~ 1 mm away from the cantilever in the Z-axis. B) Screen capture of the video camera for the situation sketched in A; the mica surface is unfocused. C) Scheme of the cantilever holder and the sample stage for approaching (side view). The X- and Y- micrometer positions are moved towards the cantilever; the cantilever should be finally placed in the vicinity of the mica edge. D) Screen capture of the video camera for the situation sketched in C; the proximity to the cantilever brings mica to the same focal plane.

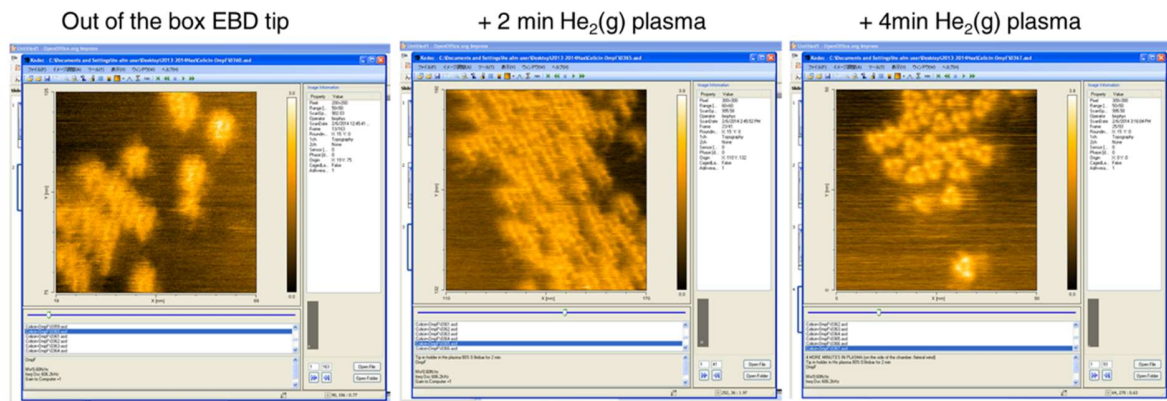


Figure 6: **Effect of Helium plasma etching on the EBD tip imaging of OmpF.** Left, Image using out of the box Nanoworld USC-F1.5-k0.6 HS-AFM probe. Central, image using the same probe after 2 minutes in Helium plasma. Right, image using the sample probe after 4 minutes in total in Helium plasma. Images are not processed.